Towards 24% efficiency for industrial n-type bifacial passivating-contact solar cells with homogeneous emitter

Jie Bao, Cheng Chen, Ronglin Liu, Zhencong Qiao, Zheren Du, Zhifeng Liu & Jia Chen, Jolywood Solar Technology Co. Ltd., Taizhou City, Jiangsu Province, China

Abstract

Passivating-contact solar cells are attracting more and more attention in the solar industry because of their high efficiency potential and high compatibility with existing passivated emitter and rear cell (PERC) and passivated emitter rear totally diffused (PERT) process flows. Jolywood was one of the first few manufacturers producing solar cells and modules featuring passivating-contact technology, with a capacity exceeding 2GW. This work reports the latest results obtained at Jolywood for full-area (251.99cm²) n-type bifacial passivating-contact solar cells using a cost-effective process with industrially-feasible boron diffusion, phosphorus ion implantation and low-pressure chemical vapour deposition (LPCVD) with in situ oxidation. The impact of a P-tail profile and a boron emitter profile on the recombination current in the non-metallized and metallized areas and the corresponding contact resistivity is systematically investigated. To the best of the authors' knowledge, a current density $J_{o,metal}$ of 666fA/cm² is the lowest value reported for a homogeneous boron emitter with a $J_{o,pass}$ of 25fA/cm². This result is an important one in order for industrial passivating-contact solar cells to be cost effective. With optimized processes, an average efficiency of up to 23.85% with an excellent open-circuit voltage V_{oc} of 703.5mV are obtained in the production line. A power loss analysis performed via Quokka3 indicates that the performance is mainly limited by the optical loss and emitter recombination. Inspired by these results, with further process optimization a record efficiency of 24.21% in R&D is achieved, featuring a V_{oc} of 711.6mV. The performance of the passivating-contact solar cells and corresponding modules is found to be stable, and sometimes even improved, under heat and light treatment, such as in standard light-induced degradation (LID) and light and elevated temperature-induced degradation (LeTID) test conditions.

Introduction

The polysilicon passivating contact has received a lot of attention from many research institutes and industries because of its excellent surface passivation and compatibility with industry-standard processes. Passivating-contact solar cells with a selective p⁺ emitter yielding 25.8% efficiency, and with an interdigitated back contact (IBC) structure yielding 26.1% efficiency, have been demonstrated by Fraunhofer ISE [1] and ISFH [2], respectively.

Inspired by those research achievements, various manufacturers, such as Jolywood, Trina Solar and GCL, have spared no effort in commercializing the passivating-contact solar cell by transferring the technology from the lab to mass production; record efficiencies of 23.85% [3], 24.79 [4], 24.58% [5] and 23.04% [6] on a full-size scale have been reported. However, achieving both low contact recombination and low contact resistivity for n⁺ poly-Si passivation is still a subject of ongoing research in industry with fire-through Ag paste.

"Achieving both low contact recombination and low contact resistivity for n⁺ poly-Si passivation is still a subject of ongoing research in industry with fire-through Ag paste."

As an n-type solar cell and module manufacturer, Jolywood focuses on the development of n-type bifacial passivating-contact solar cells, combining findings from previous developments [7,8]. An average efficiency of 23.85% and a record efficiency of 24.21% with an open-circuit voltage V_{oc} of 711.6mV have been achieved at the cell level by optimizing the doping profile of n⁺ poly-Si and p⁺ emitter. These results may provide some new guidance for cell efficiency improvements in mass production. The reliability of cells and modules is further investigated by performing light-induced degradation (LID), harsher (>3 times) LID, and light and elevated temperature-induced degradation (LeTID) tests. The results show that no degradation occurs in the cells and modules.

This paper is an extended version of a recent publication for the 37th EU PVSEC in 2020 [9].

Passivating-contact solar cell technology

Fig. 1(a) and (c) show the schematic diagram and process flow of passivating-contact solar cells processed on full-area (251.99cm²) n-type Cz substrates with a resistivity of ~1Ω·cm. The cells feature a homogeneous boron emitter with BBr_3 diffusion and tunnel-SiO_x/n⁺ poly-Si structure, doped ex situ by industrial phosphorus ion implantation. The tunnel-SiO_x is grown in situ by thermal oxidation in a low-pressure chemical vapour deposition (LPCVD) furnace and capped by intrinsic poly-Si (i-poly) of thickness greater than 100nm. The cells are screen printed with 12 busbars on both sides, as shown in Fig. 1(b).

The impacts of a phosphorus in-diffusion (P-tail) profile and a boron emitter profile on passivated current density ($J_{o,pass}$), metal recombination current density ($J_{o,metal}$) and corresponding contact resistivity (ρ_c) are systematically investigated. All of these are closely related to the performance of

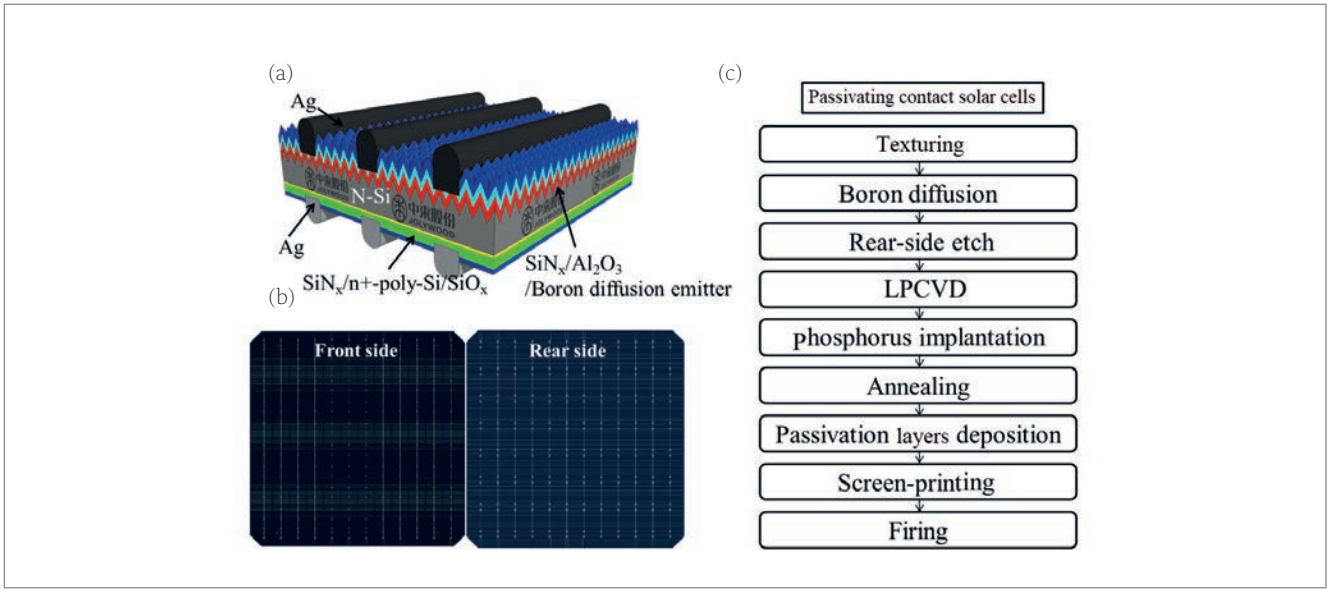

Figure 1. (a) Schematic diagram of the structure of an n-type bifacial passivating-contact solar cell. (b) Photographs of the front and rear sides of a bifacial passivating-contact solar cell fabricated at Jolywood. (c) Process sequence of a passivating-contact solar cell, used in industrial mass production.

the solar cell. The results will provide some new guidance for cell efficiency improvement in mass production and R&D.

Rear passivating-contact optimization

The rear-side SiO_x/n^+ poly-Si layers are screen printed with fire-through (FT) Ag paste. It has been reported that the FT paste could locally spike through the SiO_x/n^+ poly-Si and make contact directly with the c-Si bulk during firing, resulting in very high recombination and resistive losses [10,11]. To strike a balance between passivation and contact quality, the impact of the 'P-tail' (formed by phosphorus atoms diffusing from the n^+ poly-Si into the n-Si substrate) on surface passivation and contact properties is systematically investigated.

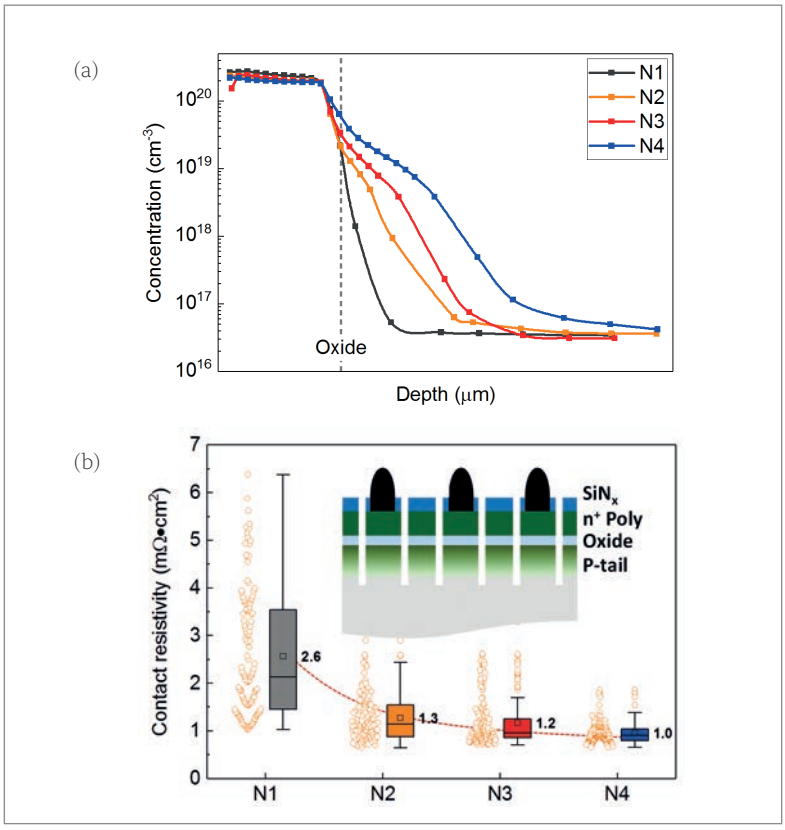

Figure 2. (a) ECV profiles for phosphorus in the tunnel-SiO_x/n^+ poly-Si structure annealed at various temperatures. (b) The corresponding contact resistivities, measured by the improved TLM structure. Inset: schematic of the improved TLM structure for the ρ_c measurement of Ag/n^+ poly-Si/SiO_x/c-Si. The dashed/dotted lines in the figure are visual guides.

As illustrated in the electrochemical capacitance–voltage (ECV) profiles in Fig. 2(a), passivating-contacts with various P-tails, marked N1–N4, are obtained by gradually increasing the annealing temperature (T_{anneal}). To avoid parasitic current flowing through several conductive layers, the n^+ poly-Si layer and P-tail in the non-contacted regions are etched before the ρ_c measurement via the transmission line method (TLM) [12] or the Cox-Strack method [13]. However, selective removal of the n^+ poly-Si layer and the P-tail is too complicated and not cost effective for industrial implementation.

To solve this problem, an improved TLM structure (see inset in Fig. 2(b)) developed by Jolywood is utilized to measure the contact resistivity of Ag/n^+ poly-Si/SiO_x/c-Si, which features a tunnel-SiO_x/n^+ poly-Si layer around each finger and which is isolated by creating grooves with a depth of more than 1.5μm in order to eliminate unwanted current paths during TLM measurements. The measured value is a 'lumped' value comprising the contact resistivity of Ag/n^+ poly-Si, the tunnel resistivity of n^+ poly-Si/SiO_x/c-Si, and the contact resistivity of the Ag/P-tail. The ρ_c values obtained via the improved TLM structure for N1–N4 are summarized in Fig. 2(b).

Fig. 2(a) reveals an initially flat distribution of P dopants in the n^+ poly-Si layer, which then drops sharply from the poly-Si/SiO_x interface (indicated by the dashed grey line) to c-Si; the P-tail within the c-Si becomes deeper as a result of more P

atoms diffusing from the poly-Si into the bulk at increasing temperatures T_{anneal}. The sample N1, with a very shallow P-tail in the Si bulk, exhibits high-quality passivation (~6fA/cm²) but poor contact performance. The upper-limit ρ_c could be around 6.5mΩ·cm².

The rear surface used in this work, formed by acid-based single-side etching, is much rougher than an alkaline polished rear surface; thus, J_o is slightly higher than for an alkaline polished surface. A moderately leaky profile, such as that exhibited by N2, with slightly more in-diffusion, helps reduce ρ_c and maintain $J_{o,pass}$ (7fA/cm²). However, as T_{anneal} continues to increase, more dopants migrate into the c-Si bulk. Although ρ_c drops further to ~1.0mΩ·cm², the value of $J_{o,pass}$ increases significantly from 14fA/cm² to 21fA/cm² (see N3 and N4 in Fig. 3).

The value of $J_{o,metal}$ is extracted by fitting $J_{o,metal}$ vs. metalization fraction, which is measured from Ag-etched lifetime samples [14]. As shown in Fig. 3, $J_{o,metal}$ drops initially with increasing T_{anneal} and gradually saturates at a similar level to that of N2. Unlike the results of Stodolny et al. [13] from ECN, $J_{o,metal}$ of the passivating contact decreases linearly with increasing in-diffusion depth. These results indicate that, in order to balance the surface recombination and contact properties, a moderate doping tail (~0.15μm) within the c-Si bulk is sufficient to avoid the high recombination and contact resistance caused by metal spikes. With the optimization, excellent passivation characteristics of a SiO_x/n^+ poly-Si structure, with $J_{o,pass}$ ~7fA/cm², $J_{o,metal}$ ~247fA/cm² and low ρ_c ~ 1.3mΩ·cm², are obtained simultaneously on a planar surface.

Front p⁺ emitter optimization

In order to find a suitable p⁺ emitter, four diffusion profiles, represented by B1–B4 with different peak concentrations (C_{peak}) and junction depths, were developed by varying the diffusion process. The doping profiles measured by ECV are depicted in Fig. 4(a); the sheet resistances of the B1–B4 profiles measured by a four-point probe (4pp) are 85, 95, 70 and 50Ω/sq., respectively. Profiles B1 and B4 initially show very similar values for C_{peak}, and likewise B2 and B3, until the junction depths for profiles B1–B4 gradually increase.

As shown in Figs. 4 and 5, the B1 profile, with a high C_{peak} and shallow junction, exhibits low non-metallized recombination ($J_{o,pass}$ ~27fA/cm²) but poor contact properties ($J_{o,metal}$ ~1,025fA/cm² and ρ_c ~2.8mΩ·cm²). The latter is attributed to the Ag-Al paste spiking too much into the p⁺ emitter (perhaps close to the p-n junction) and forming a centre of high recombination during metallization.

A high C_{peak} and a deep junction profile, such as that of B4, could provide a better shielding of the high recombination at the metal contacts ($J_{o,metal}$ ~541fA/cm²) and enable low contact resistivity (ρ_c ~0.9mΩ·cm²), while $J_{o,pass}$ is dramatically increased. A lightly doped C_{peak} and a deep junction

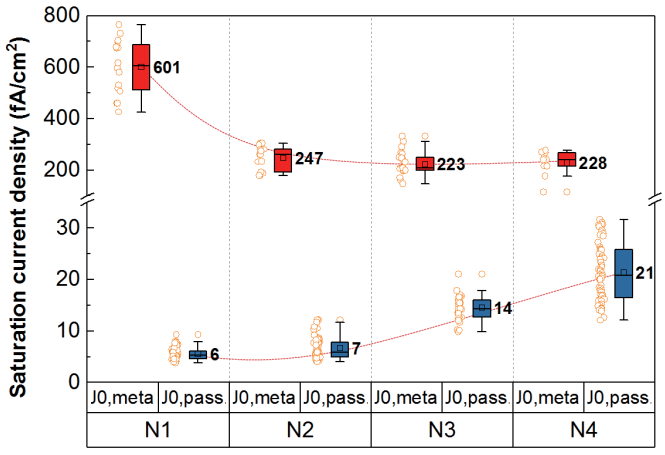

Figure 3. The corresponding non-metallized and metallized passivation properties for a passivating contact with different annealing temperatures. The dashed/dotted lines in the figure are visual guides.

"To balance the surface recombination and contact properties, a moderate doping tail within the c-Si bulk is sufficient to avoid the high recombination and contact resistance caused by metal spikes."

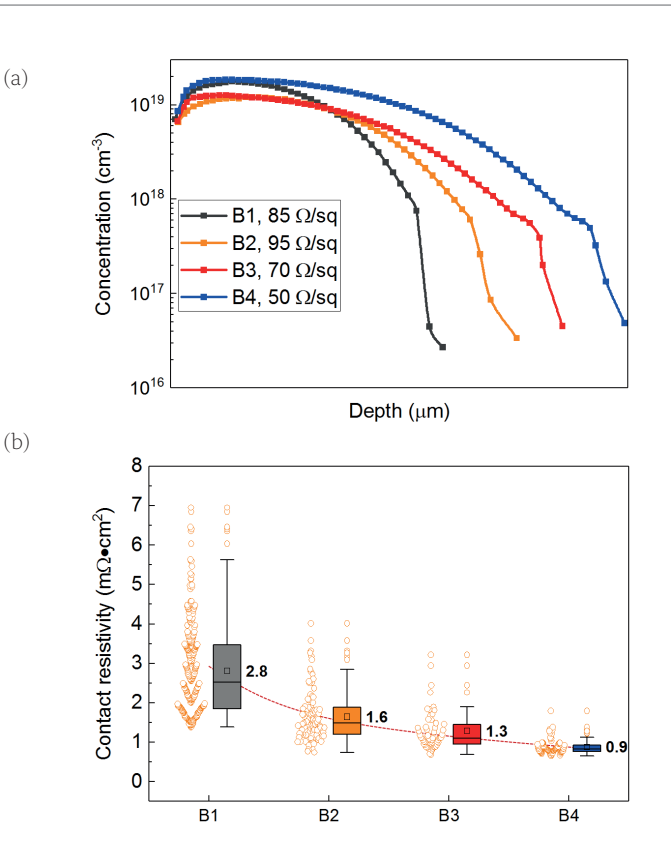

Figure 4. (a) Boron-doping profiles of the p⁺ emitter with various diffusion processes. (b) The corresponding contact resistivities are measured using the standard TLM structure. The dotted line in the figure is a visual guide.

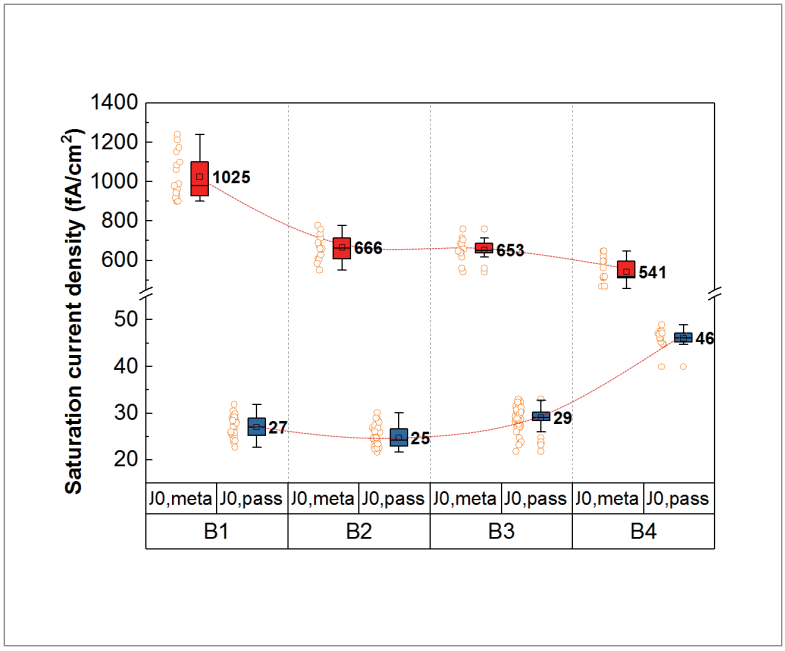

Figure 5. Corresponding passivated and metallized passivation properties for the p⁺ emitter with the doping profiles. Dashed/dotted lines in the figure are visual guides.

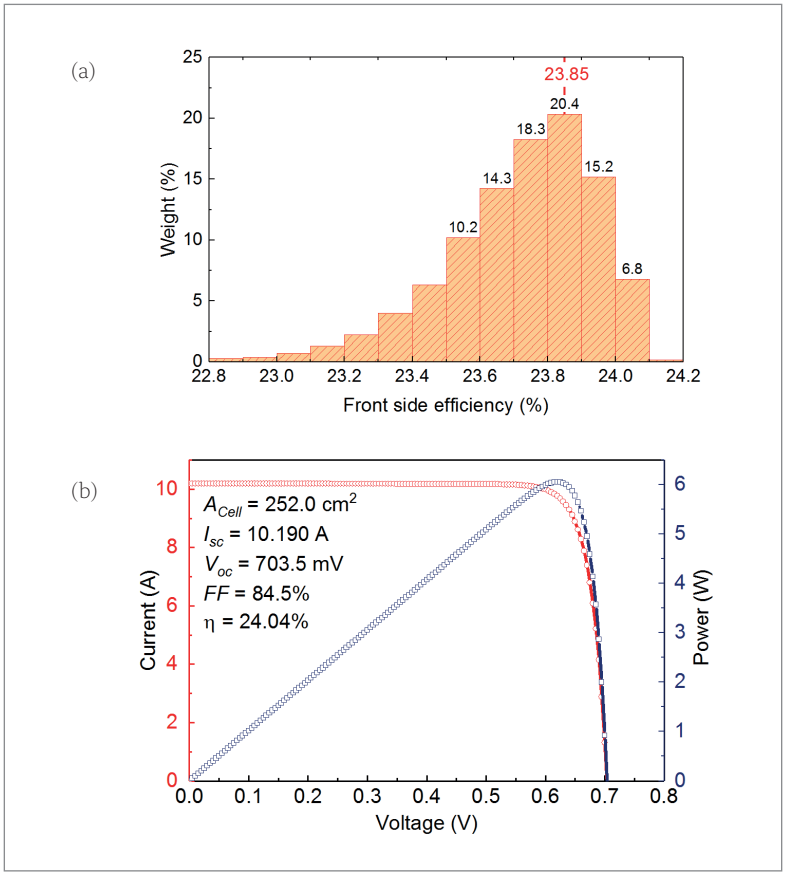

Figure 6. (a) Front-side efficiency distribution for a batch of over 20,000 cells fabricated on the production line. (b) Third-party calibrated *I–V* curves of the calibrated cell. These figures have been reproduced using the raw data.

> "The values of $J_{o,metal}$ and ρ_c of the p⁺ emitter are more related to junction depth than to peak concentration."

depth, for example demonstrated in the B2 and B3 profiles, enables both a low $J_{o,pass}$ and a low $J_{o,metal}$.

The studies carried out indicate that the values of $J_{o,metal}$ and ρ_c of the p⁺ emitter are more related to junction depth than to peak concentration. A homogeneous p⁺ emitter with a low C_{peak} and a deep junction depth is preferable in order to balance the $J_{o,pass}$, $J_{o,metal}$ and ρ_c. Compared with the B3 profile, the B2 profile shows the merits of reduced Auger recombination loss, free-carrier absorption (FCA) and lower diffusion temperature, and is therefore used in Jolywood's passivating-contact solar cells.

Mass-produced passivating-contact cells

The distribution of the front-side efficiency for a batch of 20,000 solar cells in a single production line is shown in Fig. 6, which features a very narrow efficiency distribution and thus good process stability. The average efficiency in mass production is 23.85%. The record cell in Jolywood's production line was independently measured by a third party to have a front-side efficiency of 24.04% and a V_{oc} of 703.5mV; detailed parameters are summarized in Table 1.

Power loss of the passivating-contact cell

To identify options for further improvement of cell performance, a power loss analysis of the record solar cell is performed by applying the FELA [15] approach implemented in Quokka3. As shown in Fig. 7, with the help of a passivating contact the recombination and resistive losses for the SiO_x/n⁺ poly-Si are minor. The optical loss, on the other hand, reduces the efficiency by about 2.93%, which is mostly dominated by the imperfect light-trapping loss (1.55%). After the optical loss, the p⁺ emitter is the second largest component (1.13%), among which the passivated recombination of the p⁺ emitter contributes the most (0.59%).

Enlightened by the power loss analysis, further optimization of the optical losses (such as reflection, electrode shading and light-trapping losses) was carried out. Upon incorporating a better optimized p⁺ emitter and rear n⁺ poly-Si/SiO_x into the cells, a record passivating-contact solar cell with 24.21% efficiency and 711.6mV V_{oc} was achieved.

	J_{sc} [mA/cm²]	V_{oc} [mV]	*FF* [%]	η [%]
Calibrated*	40.44	703.5	84.5	24.04

*Independently confirmed by the third-party Metrology Institute.

Table 1. Record efficiency of an n-type passivating-contact solar cell in mass production.

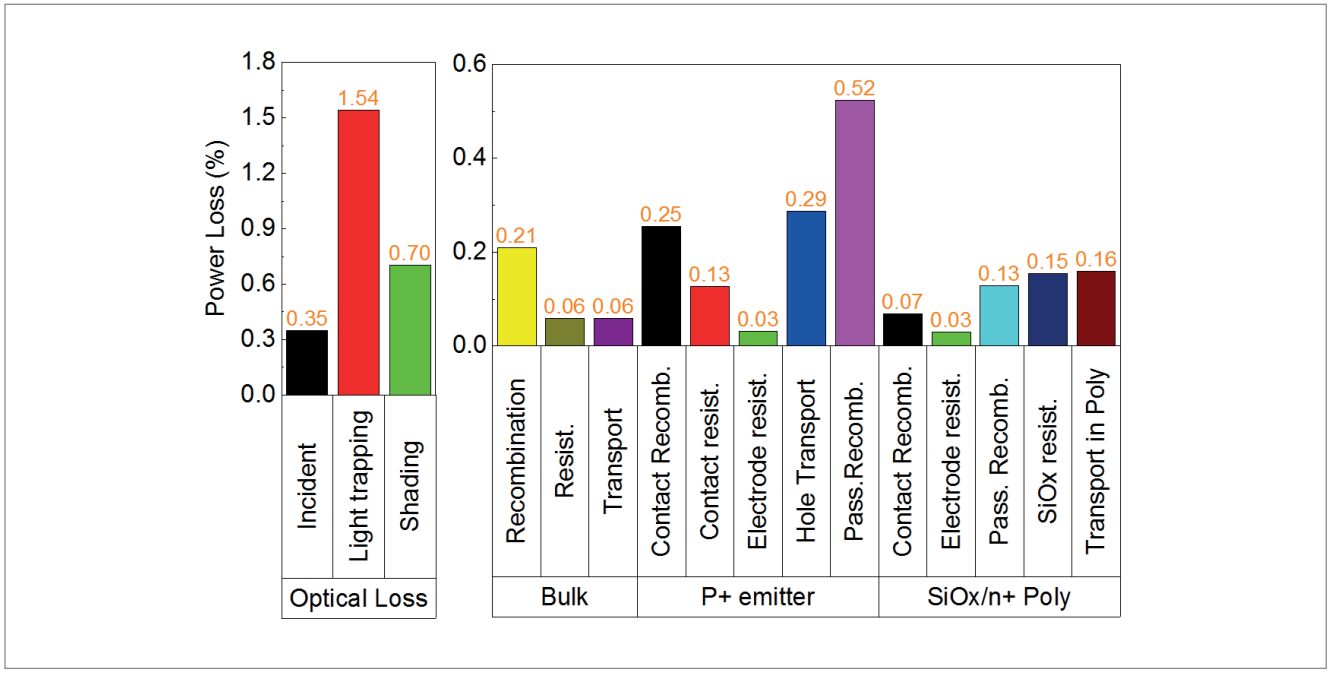

Figure 7. Detailed power loss analysis for the solar cells in mass production with an average efficiency of 23.85%.

Passivating-contact module technology

N-type modules, as shown in Fig. 8, were fabricated with Jolywood's passivating-contact silicon solar cells. A front-side *I–V* measurement was performed under standard test conditions (STC) with the rear side covered by a non-reflective black mask. Average output powers of 415W and 420W were obtained for the n-type bifacial passivating-contact modules with 72 full-size cells and 144 half-cut cells, respectively. The bifacial modules show the merits of a high bifaciality of ~85%, a low degradation coefficient of less than –1.0% for the first year and –0.4% annually thereafter, a low temperature coefficient of –0.32%/K, and a high weak-illumination response.

A full-black module developed by Jolywood utilizing a black backsheet on the rear side is shown in Fig. 8(c). Compared with a double-glass module, the weight can be reduced by ~30% by replacing the rear glass with a black backsheet. The full-black module features excellent aesthetics and light weight, which is perfect for building-integrated PV (BIPV) applications.

Reliability of passivating-contact cells and modules

LID test

In the production line, cells are randomly selected to monitor the LID after the *I–V* measurement. The test conditions for LID are five hours light soaking under 1-sun light intensity at 55°C. The relative efficiency variation is defined by $(\eta_{before} - \eta_{after})/\eta_{before}$, where η_{before} is the initial efficiency of cells before the LID test, and η_{after} is the final efficiency of the cells after the LID test.

The relative efficiency variation results for the whole of 2019 for Jolywood's bifacial passivating-contact solar cells tested under LID conditions are summarized in Fig. 9. The relative efficiency changes are all negative for n-type passivating-contact solar cells, which indicates that rather than degrading the initial efficiency, the LID test treatment is beneficial in terms of improving the efficiency of these types of solar cell.

> "Upon incorporating a better optimized p$^+$ emitter and rear n$^+$ poly-Si/SiO$_x$ into the cells, a record passivating-contact solar cell with 24.21% efficiency and 711.6mV V_{oc} was achieved."

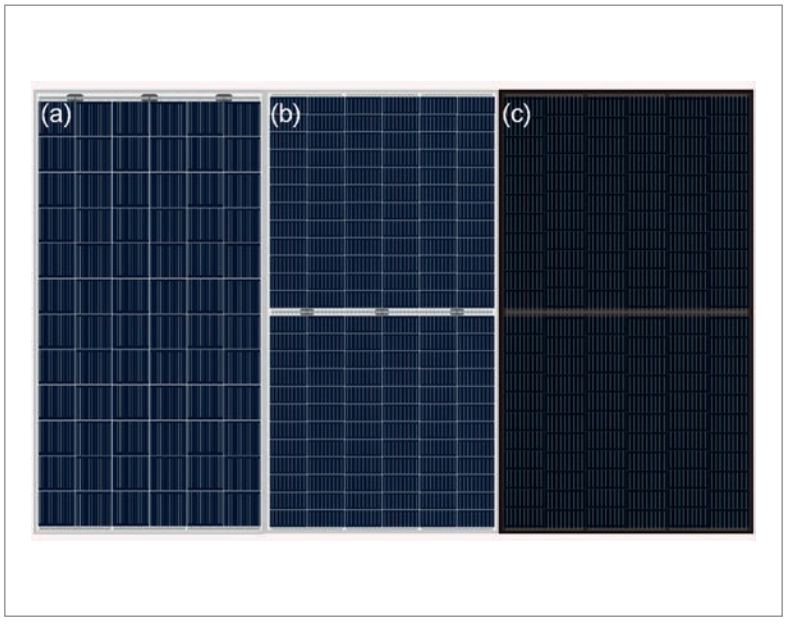

Figure 8. Images of n-type bifacial passivating-contact module products with (a) 72 full-size cells, and (b) 144 half-cut cells. (c) Full-black monofacial module with 132 half-cut cells.

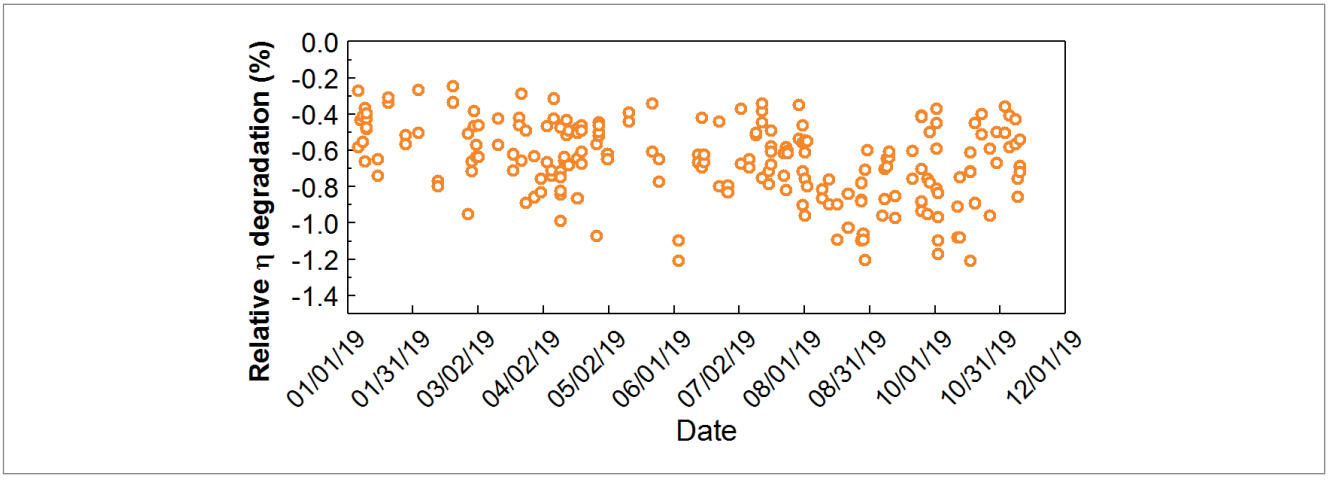

Figure 9. Light-induced degradation (LID) of n-type passivating-contact solar cells, using an illumination intensity of 1 sun and a cell temperature of 55°C.

Harsher LID test

The reliability of n-type passivating-contact solar cells is tested under much harsher conditions, such as higher temperatures (≥220°C) and higher illumination intensities (≥5 suns). This test equates to more than three times more severe than a typical LID test.

Fig. 10 shows the variation in the *J–V* parameters of the cells before and after the harsher LID test. It can be seen that after being processed with the harsher LID test, the efficiency of the cells increased by 0.17%, which is mainly due to the improvement in V_{oc} and *FF*. Consequently, the n-type passivating-contact solar cells exhibit excellent reliability, even under more stringent LID tests.

LeTID test

LeTID tests are performed on n-type bifacial passivating-contact modules with 72 full-size cells. The modules are treated in the dark chamber at 75°C with 1A current soaking, each LeTID cycle lasting 96 hours. Modules utilizing cells without having undergone the severe LID test show non-degradation after the first cycle of the LeTID test, and minor degradation (<1.0%) after the third cycle. The performance of the modules recovered and showed positive gains after the 4th cycle, as shown in Fig. 11(a). For those modules using solar cells processed with the harsher LID test, no degradation was observed, even after four cycles of the LeTID test, as shown in Fig. 11(b).

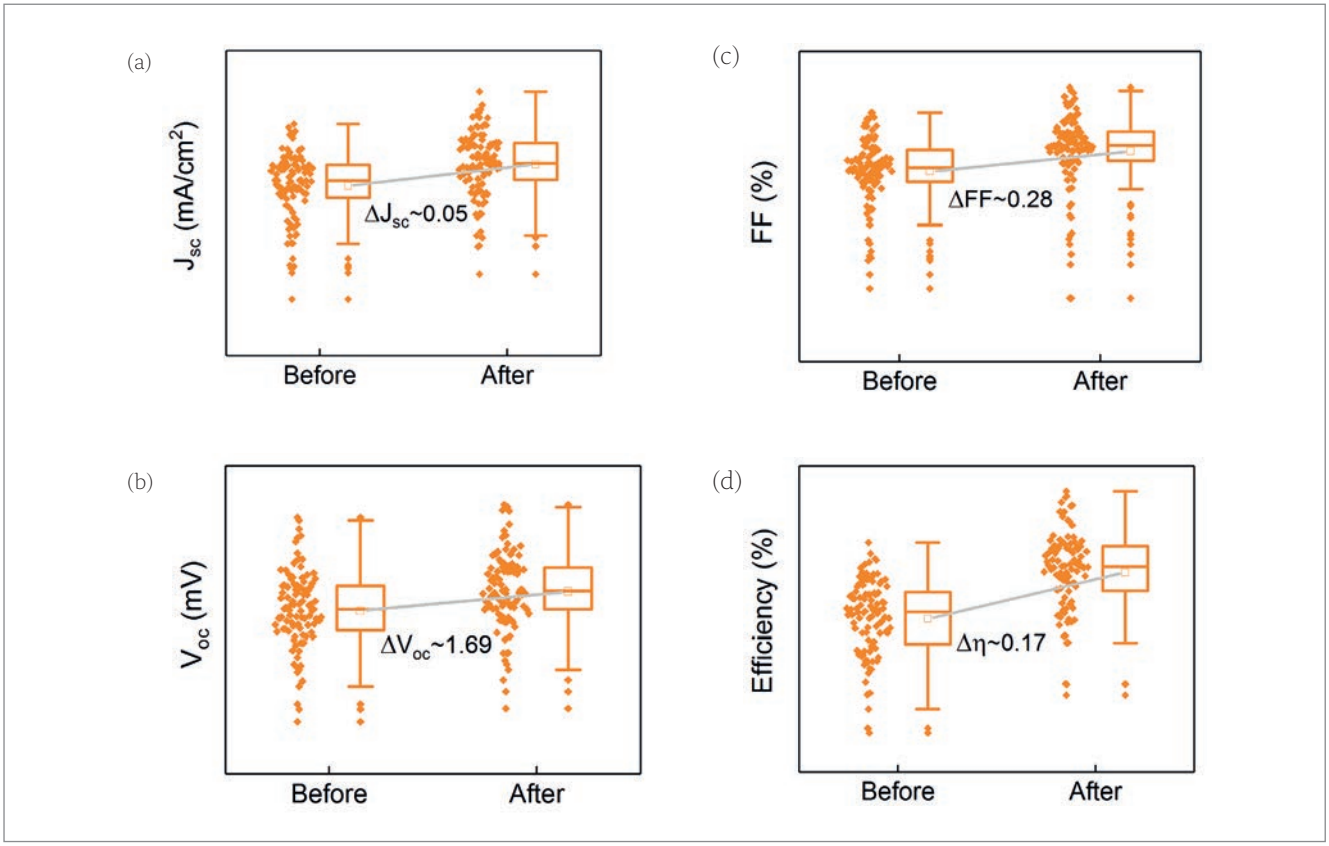

Figure 10. *J–V* parameters for n-type passivating-contact solar cells before and after the harsher (>3 times) LID tests.

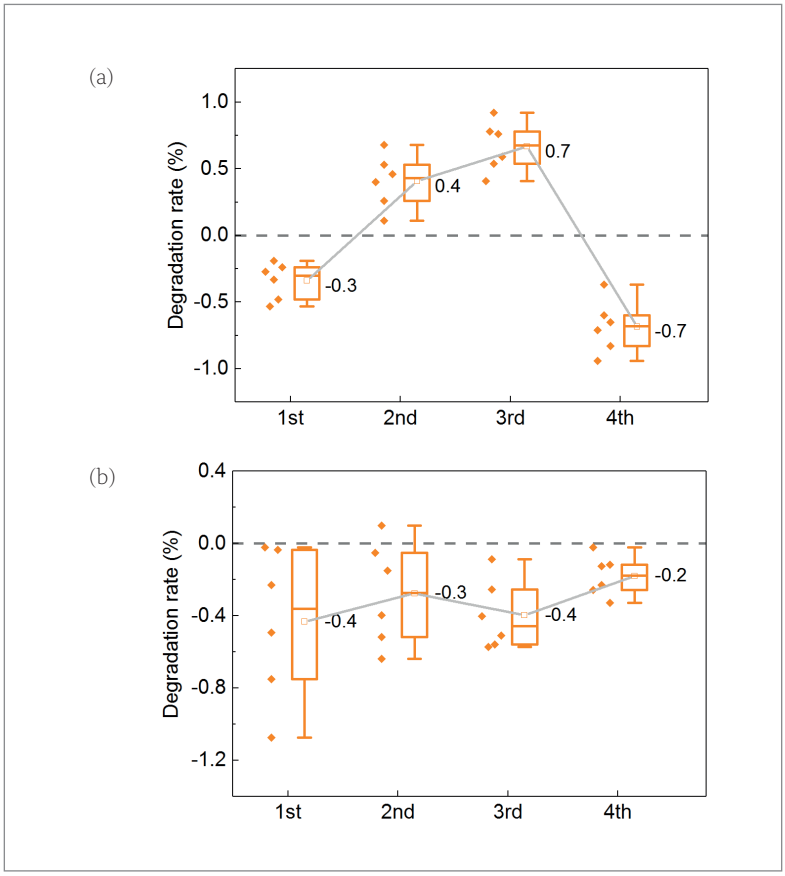

Figure 11. Four-cycle LeTID test for n-type passivating-contact modules: (a) without and (b) with the harsher (>3 times) LID test. The time duration of one cycle of the LeTID test is 96 hours, with a module temperature of 75°C and a 1A current soaking.

"The reliability tests showed that n-type bifacial passivating-contact solar cells and modules are free from LID and are minimally impacted by LeTID."

It is interesting to observe that modules treated under severe LID test conditions are more stable throughout these four cycles. It is proposed that excess hydrogen in the bulk silicon after the firing process can form hydrogen-bonded defects during the first cycle of the LeTID test. These defects, however, can be dissociated during long-duration carrier injection and annealing, which accounts for the recovery of modules after the fourth cycle. On the other hand, if the modules have already been subjected to the harsher (>3 times) LID test, the excess hydrogen in the bulk silicon becomes depleted, which keeps the solar cells in the modules free from hydrogen-related degradation in the subsequent LeTID test.

Summary

This paper has reported the latest results obtained at Jolywood for full-size n-type bifacial passivating-contact solar cells using cost-effective processes comprising phosphorus ion implantation and LPCVD with in situ oxidation. In this work, the impact of a P-tail profile and boron emitter profile on the recombination currents in the non-metalized and metallized areas and the corresponding contact resistivity were systematically investigated.

The results indicated that a moderate doping tail (~0.15μm) within the c-Si bulk in a passivating contact is sufficient to avoid the high recombination and contact resistance caused by metal spikes, and that a homogeneous p^+ emitter with low peak concentration and deep junction depth is preferred in order to balance the passivation and contact performance. With optimized fabrication processes, an average efficiency of up to 23.85% with an excellent V_{oc} of 703.5mV was obtained in the production line.

An implementation of the FELA approach in Quokka 3 revealed that optical factors (2.93%) are responsible for the largest power loss, and that recombination and resistive losses at the p^+ emitter are the second largest limitation for the record cell. With further process optimization, the best record efficiency in R&D of 24.21% was achieved, featuring a V_{oc} of 711.6mV.

The reliability tests showed that n-type bifacial passivating-contact solar cells and modules are free from LID and are minimally impacted by LeTID, which consisted of light/current soaking and annealing. Rather than degrading performance, the light soaking and annealing processes have a positive effect on V_{oc} and *FF*, which contribute to an improvement in efficiency of n-type bifacial passivating-contact solar cells and modules.

References

[1] Richter, A. et al. 2019, "Both sides contacted silicon solar cells: Options for approaching 26% efficiency", *Proc. 36th EU PVSEC*, Marseille, France, pp. 90–95.

[2] Haase, F. et al. 2018, "Laser contact openings for local poly-Si-metal contacts enabling 26.1%-efficient POLO-IBC solar cells", *Sol. Energy Mater. Sol. Cells*, Vol. 186, pp. 184–193.

[3] Chen, J. et al. 2020, "Progress and application of the new generation n-type TOPCon technology", Presentation at 14th SNEC, Shanghai, China.

[4] JinkoSolar 2020, "JinkoSolar's large-area n-type monocrystalline silicon single junction cell has a conversion efficiency of 24.79%, a world record", News report [http://www.jinkosolar.com/site/newsdetail/815].

[5] Chen, D. et al. 2020, "24.58% total area efficiency of screen-printed, large area industrial silicon solar cells with the tunnel oxide passivated contacts (i-TOPCon) design", *Sol. Energy Mater. Sol. Cells*, Vol. 206, 110258.

[6] Sheng, J. et al. 2019, "Impact of phosphorus diffusion on n-type poly-Si based passivated contact silicon solar cells", *Sol. Energy Mater. Sol. Cells*, Vol. 203, 110120.

[7] Chen, J. et al. 2019, "The development of n-type bifacial silicon solar cell and module with passivating-contact technology in Jolywood", Presentation at 9th Silicon PV, Leuven, Belgium.

[8] Wu, W. et al. 2019, "Development of industrial n-type bifacial TOPCon solar cells and modules",

Proc. 36th EU PVSEC, Marseille, France, pp. 100–102.
[9] Bao, J. et al. 2020, "Towards 24% efficiency for industrial n-type bifacial passivating-contact solar cells with homogeneous emitter", *Proc. 37th EU PVSEC* (virtual event), pp. 160–163.
[10] Çiftpınar, H. et al. 2017, "Study of screen-printed metallization for polysilicon based passivating contacts", *Energy Procedia*, Vol. 124, pp. 851–861.
[11] Padhamnath, P. et al. 2019, "Metal contact recombination in monoPoly™ solar cells with screen-printed & fire-through contacts", *Sol. Energy Mater. Sol. Cells*, Vol. 192, pp. 109–116.
[12] Rienäcker, M. et al. 2016, "Junction resistivity of carrier-selective polysilicon on oxide junctions and its impact on solar cell performance", *IEEE J. Photovolt.*, Vol. 7, No. 1, pp. 11–18.
[13] Stodolny, M. et al. 2019, "Poly-Si contacting with second generation FT pastes and accurate characterization of contact resistances", Presentation at 8th Worksh. Metalliz. Interconn. Cryst. Sil. Sol. Cells, Konstanz, Germany.
[14] Liu, R. et al. 2019, "Metal contact performance optimization of n-type passivating-contact solar cells", Presentation at 15th CSPV, Shanghai, China.
[15] Brendel, R. et al. 2008, "Theory of analyzing free energy losses in solar cells", *Appl. Phys. Lett.*, Vol. 93, 173503.

About the Authors

Jie Bao received his master's degree in optical engineering in 2017 from the Institute of Solar Energy Systems (ISES), Sun Yat-Sen University (SYSU). After graduating in 2017, he joined the Solar Cell R&D Center at Jolywood as a senior engineer. His research focuses on fabrication, characterization and simulation of n-type high-efficiency solar cells.

Cheng Chen studied physical electronics at Nanjing University of Science and Technology, China. In 2017 he joined Jolywood's R&D department as a senior engineer, focusing on the technology development, process integration and mass-production introduction of n-TOPCon solar cells.

Ronglin Liu studied microelectronics at Jiangnan University and received his master's degree in semiconductor device physics in 2009. In 2010 he started his career in the PV industry as an R&D engineer and focused on the industrialization of silicon solar cells. He joined Jolywood in 2015, where he initially focused on technology development and industrialization of n-PERT and n-TOPCon cells. Now, as an R&D manager, he leads the high-efficiency n-TOPCon team, working on efficiency optimization.

Zhencong Qiao studied condensed state physics at Henan University and received his master's degree in 2011. Later that year, he began working in the PV industry and focused on the industrialization of crystalline silicon. In 2016 he joined Jolywood, specializing in passivation and reliability of n-PERT and n-TOPCon cells. Now as an R&D manager, he leads the team involved in equipment and mass production of n-TOPCon solar cells.

Dr. Zheren Du received his bachelor of electrical engineering degree (Hons.) from the National University of Singapore (NUS) in 2010. He obtained his Ph.D. from the Department of Electrical and Computer Engineering at NUS and the Solar Energy Research Institute of Singapore (SERIS). He currently works for Jolywood, where he is in charge of the cell R&D department. His research interests include architecture, process, materials and laser processing applications in high-efficiency silicon-based solar cells.

Dr. Zhifeng Liu received his Ph.D. in the field of condensed matter physics from Nanjing University (NJU). In 2016 he was appointed director of the R&D Center, where he developed the industrialization-feasible process for IBC, n-PERT, n-TOPCon solar cells and modules. He founded and chaired the 2.4GW-capacity n-type bifacial solar cells factory. He is currently the deputy general manager of Jolywood, responsible for technology, overseas sales and marketing.

Dr. Jia Chen obtained his Ph.D. from the National University of Singapore. In 2014 he joined imec in Belgium, focusing on efficiency improvement of n-type silicon solar cells. Since 2018 he has been working at China-based Jolywood as the deputy general manager, responsible for R&D development of n-type cells and modules, such as TOPCon and IBC cell and module technologies.

Enquiries

Jia Chen
Jolywood Solar Technology Co. Ltd.
No. 6 Kaiyang Rd.
Jiangyan Economic Development Zone
Taizhou City, Jiangsu Province
China, 225500

Tel: +86 13852664642
Email: chenjia@jolywood.cn